

Diffusion Versus Advective Rearrangement of a Circular Vortex Sheet

JAMES P. KOSSIN

Cooperative Institute for Meteorological Satellite Studies, University of Wisconsin—Madison, Madison, Wisconsin

WAYNE H. SCHUBERT

Department of Atmospheric Science, Colorado State University, Fort Collins, Colorado

11 March 2002 and 27 August 2002

1. Introduction

Tropical cyclone modeling has now advanced to a stage where it is possible to predict, using three-dimensional nonhydrostatic nested-grid models, not only the synoptic-scale flow patterns that determine the cyclone track, but also the mesoscale inner core vorticity structures that determine the maximum wind and minimum central pressure (Chen and Yau 2001; Braun 2002). An observational basis for understanding the inner core vorticity structure was recently provided by Kossin and Eastin (2001), who used aircraft data to show that annular rings of high vorticity are generated in the hurricane eyewall during intensification but are typically eradicated when intensification stops. During prolonged periods of intensification, eyewall flows appear to evolve toward vortex sheets, in agreement with the theoretical notion that the dynamics of the eyewall are frontogenetic and that there is a tendency for the azimuthal flow to evolve toward a discontinuity (Emanuel 1989, 1997). Motivated by such observed flow fields in hurricanes, a theoretical and modeling study by Schubert et al. (1999) considered the barotropic stability and nonlinear evolution of unforced “hollow-tower” vorticity structures. Such structures are characterized by annular rings of enhanced vorticity (representing the eyewall) surrounding a region of relatively weak vorticity (representing the eye). Their study suggests that remarkable vorticity rearrangement processes are occurring in the inner core regions of tropical cyclones, and that these processes can have a significant effect on the structure, intensity, and evolution of the storms. Thus the simultaneous simulation of tropical cyclone

track and inner core intensity remains a challenge, at least partly because of the very different, but comparably important, horizontal scales involved. In particular, it is quite possible to incorporate horizontal diffusion in such a way that it has little effect on the scales of motion involved in track prediction but has a dominant effect on the inner core vortex structure.

The purpose of this note is to illustrate the effects of diffusion on hollow-tower vorticity structures and to determine how small a value of viscosity we should specify in three-dimensional hurricane models in order that diffusion does not erroneously dominate the advective vorticity rearrangement process. We will also comment on some of the problems associated with the use of horizontal diffusion as a parameterization of the advective vorticity rearrangement process.

2. Diffusive evolution of a circular vortex sheet

First consider the effect of horizontal diffusion on a circular vortex. The governing equation for the relative vorticity $\zeta(r, t)$ is

$$\frac{\partial \zeta}{\partial t} = \nu \frac{\partial}{\partial r} \left(r \frac{\partial \zeta}{\partial r} \right), \quad (1)$$

where ν is the kinematic viscosity. As the initial condition, consider a vortex that is initially characterized by an infinitesimally thin annular ring of enhanced vorticity embedded in an irrotational flow. The initial azimuthal wind profile is given by $v(r, 0) = 0$ for $0 \leq r < a$, and $v(r, 0) = v_0(a/r)$ for $a \leq r < \infty$, where v_0 is the initial maximum wind. This describes a circular vortex “sheet” with radius $r = a$.

One of several methods available to solve (1) is the method of Hankel transforms. The Hankel transform of $\zeta(r, t)$ is given by $\hat{\zeta}(k, t) = \int_0^\infty \zeta(r, t) J_0(kr) r dr$, and the inverse transform is given by $\zeta(r, t) = \int_0^\infty \hat{\zeta}(k, t) J_0(kr) k$

Corresponding author address: Dr. James P. Kossin, Cooperative Institute for Meteorological Satellite Studies, University of Wisconsin—Madison, Madison, WI 53706.
E-mail: kossin@ssec.wisc.edu

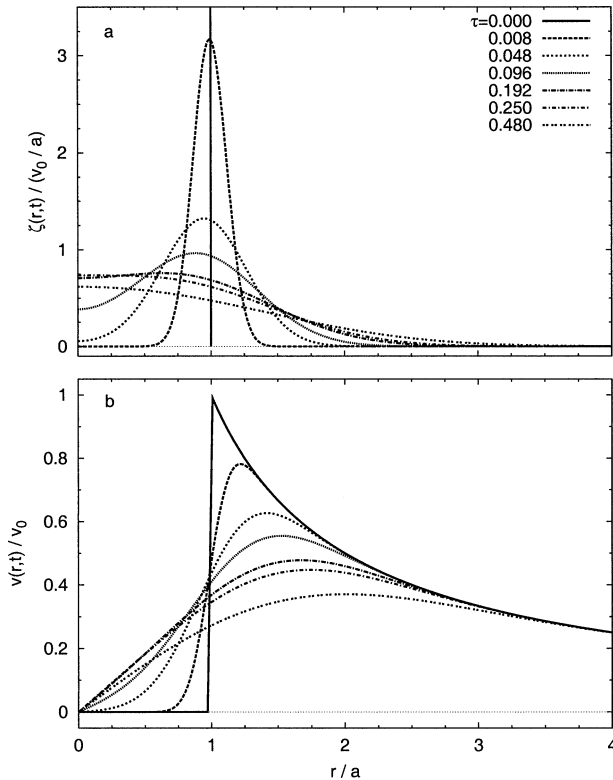


FIG. 1. Evolution of (a) nondimensional vorticity $\zeta/(v_0/a)$ and (b) nondimensional tangential wind v/v_0 based on the solution (3) for chosen values of nondimensional time $\tau = \nu t/a^2$.

dk , where J_0 is the zero-order Bessel function and k is the radial wavenumber. Applying the transform to (1), integrating by parts twice, and using the zero-order Bessel equation $rd/dr[rdJ_0(kr)/dr] = -k^2r^2J_0(kr)$, we obtain $d\hat{\zeta}/dt = -\nu k^2\hat{\zeta}$, the solution of which is given by $\hat{\zeta}(k, t) = \hat{\zeta}(k, 0) \exp(-\nu k^2 t)$. Substituting this last result into the inverse transform gives $\zeta(r, t) = \int_0^\infty \hat{\zeta}(k, 0) \exp(-\nu k^2 t) J_0(kr) k dk$, where $\hat{\zeta}(k, 0) = \int_0^a \zeta(r, 0) J_0(kr) r dr = \int_{a-\varepsilon}^{a+\varepsilon} \{d[r\nu(r, 0)]/dr\} J_0(kr) dr = av_0 J_0(ka)$ in the limit $\varepsilon \rightarrow 0$. Using these last two results we obtain

$$\zeta(r, t) = av_0 \int_0^\infty J_0(ka) \exp(-\nu k^2 t) J_0(kr) k dk, \quad (2)$$

which is an integral representation for the solution of our diffusion problem. The integral in (2) can be evaluated (see Gradshteyn and Ryzhik 1994, p. 739) to obtain

$$\zeta(r, t) = \frac{v_0/a}{2\tau} \exp\left\{-\left[\frac{(r/a)^2 + 1}{4\tau}\right]\right\} I_0\left(\frac{r/a}{2\tau}\right), \quad (3)$$

where I_0 is the modified Bessel function of order zero, and $\tau = \nu t/a^2$ is a dimensionless time.

Figure 1a, which has been constructed using (3), shows plots of the dimensionless vorticity $\zeta(r, t)/(v_0/a)$ as a function of r/a for seven different values of the dimensionless time τ . To construct the corresponding

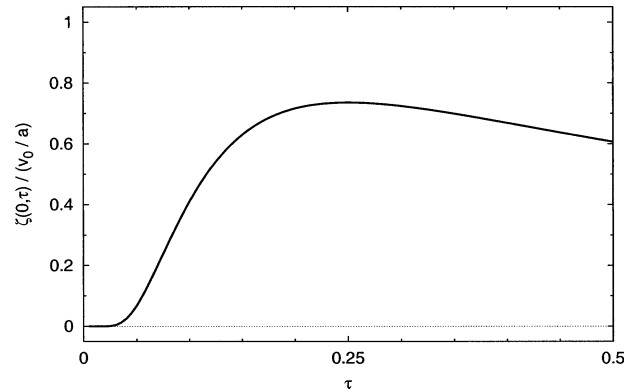


FIG. 2. Evolution of nondimensional vorticity $\zeta/(v_0/a)$ at $r = 0$ as a function of nondimensional time $\tau = \nu t/a^2$.

wind plots shown in Fig. 1b we have used numerical quadrature on $v(r, t) = r^{-1} \int_0^r \zeta(r', t) r' dr'$ with the integrand $\zeta(r', t) r'$ computed using (3). Figure 1 shows how the diffusive flux of vorticity smooths the profiles and drives the vorticity from a hollow-tower to a monotonic profile. The tangential wind profile becomes increasingly less “U shaped” as the flow increases in the eye and decreases in the eyewall.

For $r = 0$ and $t > 0$, (3) reduces to $\zeta(0, \tau) = (v_0/a)[1/(2\tau)] \exp[-1/(4\tau)]$, from which we can plot the dimensionless central vorticity $\zeta(0, \tau)/(v_0/a)$ as a function of τ . This is shown in Fig. 2. The central flow remains approximately irrotational until $\tau \approx 0.03$, after which the central vorticity increases until it achieves its maximum at $\tau = 0.25$. When $\tau = 0.25$, the Laplacian operator on the right-hand side of (1), evaluated at $r = 0$, vanishes, and the central vorticity is $(2v_0/a)e^{-1}$, that is, e^{-1} times the initial average vorticity inside $r = a$. When $\tau > 0.25$ the central vorticity decreases as all the diffusive flux is then directed outward. The increase of the central vorticity due to the inward flux when $\tau < 0.25$ is much more rapid than the “slow diffusive spin-down” that occurs later. In other words, the diffusion is more efficient at eradicating the annular ring than the subsequent monopole. Since $\tau = 0.25$ is the dimensionless diffusive time to monopole formation, we can define the dimensional diffusive time to monopole formation as $t_{mf} = a^2/(4\nu)$. For $a = 10$ km, t_{mf} is, respectively, 694, 69.4, and 6.94 h for $\nu = 10, 100,$ and 1000 $\text{m}^2 \text{s}^{-1}$, a range of eddy viscosity values typically used in hurricane models.

3. Advective–diffusive evolution of a circular vortex sheet

With the choice $a = 10$ km, the vorticity and wind profiles at $\tau = 0.008$ in Fig. 1 are very similar to the initial condition used by Kossin and Schubert (2001) in experiment 7 of their vorticity mixing study. In their results, reproduced here in Fig. 3, the initial annular ring of vorticity advectively rearranges itself into a vor-

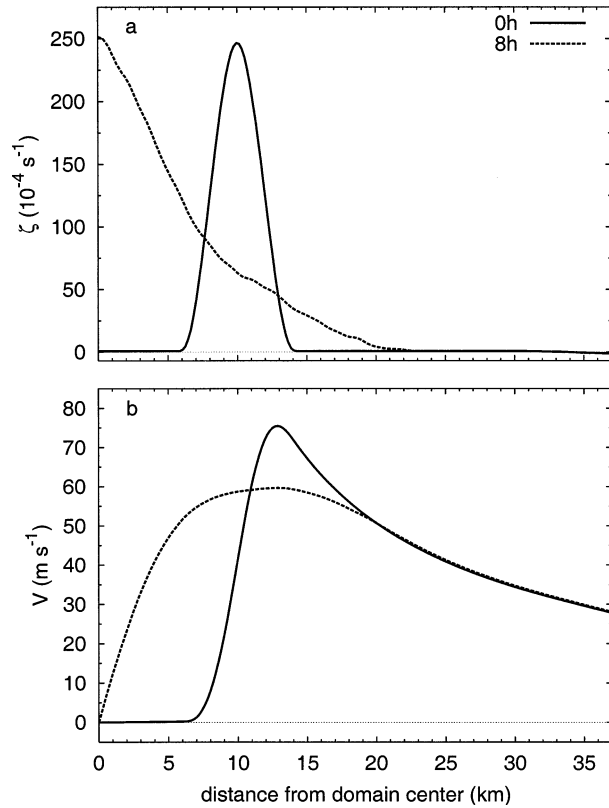


FIG. 3. Azimuthal mean (a) vorticity and (b) tangential wind at $t = 0$ and after an 8-h numerical integration of (4). Reproduced from Kossin and Schubert (2001, their Fig. 11).

ticity monopole in less than 8 h, according to the non-divergent barotropic dynamics:

$$\zeta_t + u\zeta_x + v\zeta_y = \nu\nabla^2\zeta, \quad (4)$$

where $u = -\psi_y$, $v = \psi_x$, and $\zeta = \nabla^2\psi$. Their results are nearly inviscid since their specified viscosity is $\nu = 5 \text{ m}^2 \text{ s}^{-1}$, which gives a dimensional diffusive time to monopole formation of $t_{\text{mf}} = a^2/(4\nu) \approx 1389 \text{ h}$, much longer than the roughly 7 h required for advective rearrangement to a monopole. Values of ν somewhat larger than $\nu = 5 \text{ m}^2 \text{ s}^{-1}$ would also seem acceptable. For example, $\nu = 100 \text{ m}^2 \text{ s}^{-1}$ gives $t_{\text{mf}} = 69.4 \text{ h}$, which is about 10 times the time required for advective rearrangement.

Now suppose we want to parameterize the asymmetric advective rearrangement process in an axisymmetric model using simple diffusion. What value of ν should be used? If we want the timescale of monopole formation to be correctly parameterized in the axisymmetric model, we should choose ν to satisfy $\nu = a^2/(4t_{\text{mf}}) = (10 \text{ km})^2/(4 \times 7 \text{ h}) \approx 1000 \text{ m}^2 \text{ s}^{-1}$. However, this simple parameterization has serious deficiencies since, during the advective process, the peak value of vorticity remains unchanged (see Fig. 3), while during the pure diffusive process illustrated in Fig. 1, the peak vorticity at $\tau = 0.25$ is only 24% of the peak value at

$\tau = 0.008$. It is in this regard that the results of advective rearrangement and the results of diffusion are quite different. We can summarize by saying that the purely diffusive evolution of an annular ring does not accurately parameterize the process of vorticity rearrangement, particularly in the hurricane inner core.

Another way to interpret the basic difference between advective rearrangement of vorticity and simple diffusion of vorticity is in terms of the selective decay principle of 2D turbulence theory. This principle states that in two-dimensional high Reynolds number flows, governed by (4), the global enstrophy $Z = \iint \frac{1}{2}\zeta^2 dx dy$ is selectively decayed over the global kinetic energy $\mathcal{E} = \iint \frac{1}{2}(u^2 + v^2) dx dy$. This is a consequence of the fact that, according to the governing dynamics (4), $\mathcal{E}(t)$ and $Z(t)$ obey $d\mathcal{E}/dt = -2\nu Z$ and $dZ/dt = -2\nu\mathcal{P}$, where $\mathcal{P} = \iint \frac{1}{2}\nabla\zeta \cdot \nabla\zeta dx dy$ is the global palinstrophy, a measure of the overall vorticity gradient. Global palinstrophy evolution is described by

$$\begin{aligned} \frac{d\mathcal{P}}{dt} = & - \iint [u_x\zeta_x^2 + (v_x + u_y)\zeta_x\zeta_y + v_y\zeta_y^2] dx dy \\ & - \nu \iint (\nabla^2\zeta)^2 dx dy. \end{aligned} \quad (5)$$

Although the last term in (5) always tends to reduce \mathcal{P} , during the advective rearrangement of vorticity, \mathcal{P} can rapidly increase due to the first term on the right-hand side of (5), and for small enough values of ν , \mathcal{P} can surge to values very much larger than its initial value (cf. Schubert et al. 1999, Fig. 8). During the period of large \mathcal{P} , Z decays rapidly in comparison with \mathcal{E} , whose rate of decay becomes smaller as Z becomes smaller. In this way, Z is highly damped while \mathcal{E} is nearly invariant. This is the essence of the selective decay hypothesis. The palinstrophy evolution associated with the pure diffusive vorticity evolution described by (1) is given by $d\mathcal{P}/dt = -\nu 2\pi \int \{\partial[r(\partial\zeta/\partial r)]/(r\partial r)\}^2 r dr$, which is the nonadvective, axisymmetric, special case of (5). Thus, in the pure diffusive case, \mathcal{P} can never achieve values higher than its initial value, and the essence of the selective decay of enstrophy over energy cannot be simulated.

Although pure diffusion is not consistent with selective decay of enstrophy over energy, there are a number of parameterizations that are consistent. The anticipated vorticity method for the nondivergent barotropic model (Leith 1985), and its generalization to the shallow water equations and to the quasi-static primitive equations [referred to as the anticipated potential vorticity method (Sadourny and Basdevant 1985)] are formed by recasting the equations of motion using a modified diffusion that conserves energy exactly and allows dissipation of enstrophy or potential enstrophy. In addition, certain spatial discretization schemes (Arakawa and Hsu 1990) have been designed to mimic the anticipated potential vorticity method and thus to be consistent with selective

decay. The maximum entropy production principle (Kazantsev et al. 1998) is a statistical method that relies on solution of the variational problem of globally maximizing the rate of production of Boltzmann mixing entropy under the physical constraints of the system (e.g., global energy conservation), while allowing dissipation of enstrophy. These parameterizations could be considered an improvement over pure diffusion, but they can still suffer from deficiencies when modeling the dramatic vorticity rearrangements that can occur in the hurricane inner core. For example, the maximum entropy solutions to barotropically unstable initial flows do not capture the process whereby coherent vorticity structures are transported via advection while remaining relatively unmixed in the process (e.g., Jin and Dubin 1998) and thus the method tends to underpredict (overly mix) vorticity values.

Acknowledgments. We thank Kerry Emanuel for his comments on the original manuscript. This work was supported by NASA/CAMEX Contract NAG5-11010, NSF Grant ATM-0087072, and NOAA Grant NA67RJ0152.

REFERENCES

- Arakawa, A., and Y.-J. G. Hsu, 1990: Energy conserving and potential-enstrophy dissipating schemes for the shallow water equations. *Mon. Wea. Rev.*, **118**, 1960–1969.
- Braun, S. A., 2002: A cloud-resolving simulation of Hurricane Bob (1991): Storm structure and eyewall buoyancy. *Mon. Wea. Rev.*, **130**, 1573–1592.
- Chen, Y., and M. K. Yau, 2001: Spiral bands in a simulated hurricane. Part I: Vortex Rossby wave verification. *J. Atmos. Sci.*, **58**, 2128–2145.
- Emanuel, K. A., 1989: The finite-amplitude nature of tropical cyclogenesis. *J. Atmos. Sci.*, **46**, 3431–3456.
- , 1997: Some aspects of hurricane inner-core dynamics and energetics. *J. Atmos. Sci.*, **54**, 1014–1026.
- GradshTEyn, I. S., and I. M. Ryzhik, 1994: *Tables of Integrals, Series, and Products*. 5th ed. Academic Press, 1204 pp.
- Jin, D. Z., and D. H. E. Dubin, 1998: Regional maximum entropy theory of vortex crystal formation. *Phys. Rev. Lett.*, **80**, 4434–4437.
- Kazantsev, E., J. Sommeria, and J. Verron, 1998: Subgrid-scale eddy parameterization by statistical mechanics in a barotropic ocean model. *J. Phys. Oceanogr.*, **28**, 1017–1042.
- Kossin, J. P., and M. D. Eastin, 2001: Two distinct regimes in the kinematic and thermodynamic structure of the hurricane eye and eyewall. *J. Atmos. Sci.*, **58**, 1079–1090.
- , and W. H. Schubert, 2001: Mesovortices, polygonal flow patterns, and rapid pressure falls in hurricane-like vortices. *J. Atmos. Sci.*, **58**, 2196–2209.
- Leith, C. E., 1985: Two-dimensional coherent structures. *Proceedings of the International School of Physics "Enrico Fermi," Course 88: Turbulence and Predictability in Geophysical Fluid Dynamics and Climate Dynamics*, M. Ghil, R. Benzi, and G. Parisi, Eds., North-Holland Physics Publishing, 266–280.
- Sadourny, R., and C. Basdevant, 1985: Parameterization of subgrid scale barotropic and baroclinic eddies in quasi-geostrophic models: Anticipated potential vorticity method. *J. Atmos. Sci.*, **42**, 1353–1363.
- Schubert, W. H., M. T. Montgomery, R. K. Taft, T. A. Guinn, S. R. Fulton, J. P. Kossin, and J. P. Edwards, 1999: Polygonal eyewalls, asymmetric eye contraction, and potential vorticity mixing in hurricanes. *J. Atmos. Sci.*, **56**, 1197–1223.